Damage identification in a complex truss structure using modal characteristics correlation method and sensitivity-weighted search space

Khac-Duy Nguyen[1], Tommy HT Chan[1] David P Thambiratnam[1] and Andy Nguyen[2]

Abstract

Damage identification for complex structures is a challenging task due to large amount of structural elements, limited number of measured modes and uncertainties in referenced numerical models. This paper presents a study on enhancing the effectiveness of modal characteristics correlation methods for damage identification of complex structures. Firstly, a correlation method using change in ratio of modal strain energy-eigenvalue (MSEE change) is introduced. Damage information is determined via a forward approach by optimizing the correlation level between the patterns of the analytical and measured MSEE changes. Different from traditional optimization-based forward methods that require accurate numerical models, damage sensitivity coefficients of MSEE are directly estimated from experimental modal information. To enhance the damage identification capability, both elemental MSEE and total MSEE components are examined in the correlation function. Secondly, a sensitivity-weighted search space (SWSS) scheme incorporated with genetic algorithm (GA) is developed to overcome the ill-posed problem that causes false detection errors. Finally, the correlation method and the enhanced technique are experimentally tested on a complex truss model with nearly 100 elements. To deal with the huge number of degrees of freedom in this structure, a multi-layout roving test with the adoption of redundant channels is designed, and a three-criterion strategy is used for the selection of modes. Results demonstrate the effectiveness of the proposed damage assessment framework to locate and estimate damage in complex truss structures.

Keywords:

Damage identification, modal strain energy, correlation-based method, genetic algorithm, search space, complex truss structure.

---

[1]School of Civil Engineering and Built Environment, Queensland University of Technology, Australia
[2]School of Civil Engineering and Surveying, University of Southern Queensland, Australia

Corresponding author:
Khac-Duy Nguyen, School of Civil Engineering and Built Environment, Queensland University of Technology, 2 George St, Brisbane, QLD 4001, Australia
Email: k25.nguyen@qut.edu.au or nkduy.qut@gmail.com

Introduction

Damage identification in a structural system is a process of examining changes in measured response of the system to detect, locate and characterize damage in the system.[1] According to Rytter,[2] the damage identification process can be illustrated in four levels as follows: level 1 gives the information whether damage is present in the structure; levels 2 and 3 respectively provide information about the location and the magnitude of the damage; and level 4 evaluates the remaining life which requires a comprehensive interpretation of the impact of the discovered damage on the structure. Based on change in vibration characteristics, many damage identification methods have been developed and many of them have shown their capability to cope with level 2 and level 3 of the damage identification problem.[3-11] However, these methods have mostly been validated with numerical models or simple experimental structures. Only few studies have been conducted for complex structures.[11-13] Two probable difficulties when dealing with complex structures are the large number of degrees of freedom (DOFs) and high modelling uncertainty. In order to obtain the measures of all DOFs, mode shape expansion methods can be used but they heavily rely on the numerical model whose accuracy is not controllable due to the high modelling uncertainty. Having a dense array of sensors is more likely the solution for complex structures; however, cost associated with sensor deployment and management is a big issue. Instead of measuring all DOFs in one measurement, a sensor roving scheme can be used to overcome the equipment difficulty. Although more measurement errors might be induced, an appropriate setup of sensor layouts and an appropriate mode selection strategy can help to obtain feasible dataset for damage identification.

Truss is a common structural type and can be found in many bridges, towers, buildings and space structures. Possible damage in truss structures can be joint failure or member corrosion. Damage identification for truss structures has been previously studied by many researchers. However, most of the previous studies have been limited to numerical models or simple experimental models.[14-17] Some researchers have attempted to examine more complex truss structures but they only considered a small region of the structure to test their methodologies.[18, 19] Therefore, it will be beneficial to treat a truss with a large number of members in the damage identification study.

Regarding damage identification methods, it has been found that optimization-based forward methods are effective for locating and quantifying damage by adopting optimization techniques to solve the damage identification problem. However, one significant problem of the traditional forward methods is the requirement of an accurate numerical model.[6,7] This makes these methods to be less practical for complex structures that are usually modeled with high level of uncertainty. Recently, a novel forward method using ratio of geometric modal strain energy-eigenvalue (GMSEE) has been developed and its effectiveness and robustness have been demonstrated.[11] Compared to the traditional forward methods, the GMSEE method makes use of experimental modal parameters to estimate the change in GMSEE, and this makes it more advantageous for practical applications. However, it is noticeable that the method requires a good number of measured modes to minimize the errors caused by an erratic assumption. Further improvement in this method is needed to deal with complex structures for which only a few modes would be reliably measured.

The damage identification problem is often ill-posed due to calculation errors or other uncertainties, which leads to non-uniqueness of the solutions of damage location and severity. Salawu[20] reported that the damage identification is only reliable for elements with high strain energy since only very small change in modal parameters will be a result of a very large change in structural stiffness of low-strain-energy elements. The accuracy of damage prediction is higher for the damage occurring at sections of high modal strain amplitude than for the one at sections of low modal strain amplitude.[21] Hsu and Loh[22] conducted a damage identification study for a frame structure and reported about abnormal results at the elements with modal strain energy (MSE) close to zero. In order to avoid these false errors, they suggested a criterion for ignoring the elements with low levels of MSE. In another study for beam structures, Wahalathantri[23] considered all the structural elements and suggested to multiply the damage results by a modification function as a form of normalized MSE curve. However, this technique is only suitable for adjusting a damage location result. It is not appropriate to multiply a damage extent result by this curve as it will change the quantification.

To address the above-mentioned research needs, this paper presents a novel damage assessment framework for complex truss structures using an improved correlation-based damage identification algorithm together with an enhanced search space scheme. The original damage identification algorithm GMSEE method has been modified to better reflect the damage effect. The improved method uses change in modal strain energy-eigenvalue (MSEE) for damage identification. Also, a sensitivity-weighted search space (SWSS) scheme is introduced in which different search spaces are applied to different structural elements based on their MSEE sensitivity values. For validation, a laboratory-scaled complex truss model with nearly 100 elements is examined. A roving test with 18 accelerometers is conducted to obtain modal information of the structure, and a three-criterion approach is introduced for the selection of modes. Then, damage identification using the correlation method and the enhanced technique is performed. The effectiveness of using redundant sensors is also tested.

Theory

The previously proposed GMSEE method identifies the damage from maximizing correlation level between a measured and an analytical GMSEE change vectors. Each vector consist of the corresponding changes in elemental GMSEE for all the measured modes. The analytical change in each elemental GMSEE is calculated from the measured modal parameters (i.e., natural frequencies and mode shapes) and the elemental stiffness matrix. Different from the traditional optimization-based forward methods, the estimation of the analytical GMSEE change vector does not require numerical modes and mass-normalized mode shapes, and therefore, this method is found more feasible for practical applications. However, the estimation of this vector relies on the assumption that the fractional modal strain energy is unchanged after damage. The idea behind this assumption is that the changes in eigenvalues of the structure can be assumed to be linear to stiffness changes. This assumption is found acceptable for small damage but causes some calculation errors for large damage.[5] In order to dominate the errors caused by this assumption, a good number of modes should be used. This section presents an improved version of this method that can reduce the negative effect of the above assumption, and therefore, number of modes used can be reduced. The improved method uses modal strain energy-eigenvalue ratio (MSEE) instead of GMSEE. To enhance the damage identification capability, the method examines both elemental MSEE and total MSEE changes as the latter parameter can be estimated with higher precision.

MSEE correlation-based forward method

Sensitivity analysis for elemental MSEE. In order to estimate the change in elemental MSEE due to stiffness change, it is still assumed that the change in fractional modal strain energy is neglected. Based on the sensitivity analysis of elemental GMSEE,[11] the change in elemental MSEE can be estimated as follows:

$$\mathrm{d}W_{ij} = -\frac{U_{ij}}{\lambda_i}\mathrm{d}D_j = S_{ij}\,\mathrm{d}D_j \tag{1}$$

where $W_{ij} = U_{ij}/\lambda_i$ is the MSEE of the j^{th} element for the i^{th} mode; λ_i is the eigenvalue of the i^{th} mode; $U_{ij} = \mathbf{\Phi}_i^{\mathrm{T}}\mathbf{K}_j\mathbf{\Phi}_i$ is the MSE of the j^{th} element for the i^{th} mode, where $\mathbf{\Phi}_i$ is the measured mode shape vector of the i^{th} mode and $\mathbf{K}_j$ is the stiffness matrix of the j^{th} element; $\mathrm{d}D_j$ is the relative reduction of stiffness of the j^{th} element; and S_{ij} is the sensitivity of the MSEE of the j^{th} element for the i^{th} mode.

Sensitivity analysis for total MSEE. It should be noted that the change in elemental MSEE in Eq. (1) is a simplified expression by neglecting the change in fractional modal strain energy. The full expression for the elemental MSEE change is as follows:

$$\mathrm{d}W_{ij} = \frac{U_{ij}}{\lambda_i}\mathrm{d}F_{ij} + S_{ij}\,\mathrm{d}D_j \tag{2}$$

where $F_{ij} = \dfrac{\mathbf{\Phi}_i^{\mathrm{T}}\mathbf{K}_j\mathbf{\Phi}_i}{\mathbf{\Phi}_i^{\mathrm{T}}\mathbf{K}\mathbf{\Phi}_i}$ is the fractional modal strain energy for the j^{th} element and the i^{th} mode and $\mathbf{K}$ is the system stiffness matrix. By taking the summation in Eq. (2) for all elements, we have the change in total MSEE as follows:

$$\mathrm{d}W_i = \mathrm{d}\sum_{j=1}^{n} W_{ij} = \frac{U_{ij}}{\lambda_i}\sum_{j=1}^{n}\mathrm{d}F_{ij} + \sum_{j=1}^{n} S_{ij}\,\mathrm{d}D_j \tag{3}$$

where W_i is the total modal strain energy-eigenvalue ratio of mode i and can be obtained from measured mode shape and eigenvalue as $W_i = \mathbf{\Phi}_i^{\mathrm{T}}\mathbf{K}\mathbf{\Phi}_i/\lambda_i$. Considering a fact that the total change in fractional modal strain energy is zero ($\sum_{j=1}^{n}\mathrm{d}F_{ij} = 0$), Eq. (3) can be rewritten as follows:

$$\mathrm{d}W_i = \sum_{j=1}^{n} S_{ij}\,\mathrm{d}D_j \tag{4}$$

It is worth noting that Eq.(4) is an exact expression for the total MSEE change without considering the assumption that the change in fractional modal strain energy is neglected.

However, the total MSEE is a global parameter which is less sensitive to stiffness changes in individual structural elements. Therefore, an appropriately combined use of elemental MSEE (Eq. (1)) and total MSEE (Eq. (4)) may help to improve the damage prediction. The next section will present a combined use of these two parameters for damage identification.

Damage identification using MSEE changes. The damage identification problem can be transformed to an optimization problem using a correlation function. The multiple damage location assurance criterion (MDLAC) proposed by Messina *et al*[5] can be modified to evaluate the correlation between the measured and analytical MSEE change vectors as follows:

$$\mathrm{MDLAC}(\delta\mathbf{D}) = \frac{\left|\Delta\mathbf{MSEE}^{\mathrm{T}}.\delta\mathbf{MSEE}\right|^2}{\left(\Delta\mathbf{MSEE}^{\mathrm{T}}.\Delta\mathbf{MSEE}\right).\left(\delta\mathbf{MSEE}^{\mathrm{T}}.\delta\mathbf{MSEE}\right)} \tag{5}$$

where $\Delta\mathbf{MSEE}$ is the measured MSEE change vector including the elemental MSEE change and the total MSEE change; and $\delta\mathbf{MSEE}$ is the analytical MSEE change vector for a known damage vector $\delta\mathbf{D}$. MDLAC values range from 0 to 1, indicating correlation level from no correlation to exact correlation between the patterns of the measured and analytical MSEE changes. The damaged elements can be identified by searching the greatest MDLAC value. In this study, the genetic algorithm (GA) is utilized for this task. If m modes are used, the measured and analytical MSEE change vectors are given by the following expressions:

$$\mathbf{\Delta MSEE} = \left[\begin{Bmatrix} \mathbf{\Delta W}_1 \\ \Delta W_1 \end{Bmatrix}^{\mathrm{T}} \begin{Bmatrix} \mathbf{\Delta W}_2 \\ \Delta W_2 \end{Bmatrix}^{\mathrm{T}} \cdots \begin{Bmatrix} \mathbf{\Delta W}_i \\ \Delta W_i \end{Bmatrix}^{\mathrm{T}} \cdots \begin{Bmatrix} \mathbf{\Delta W}_m \\ \Delta W_m \end{Bmatrix}^{\mathrm{T}} \right]^{\mathrm{T}} \tag{6}$$

$$\boldsymbol{\delta}\mathbf{MSEE} = \left[\begin{Bmatrix} \boldsymbol{\delta}\mathbf{W}_1 \\ \delta W_1 \end{Bmatrix}^{\mathrm{T}} \begin{Bmatrix} \boldsymbol{\delta}\mathbf{W}_2 \\ \delta W_2 \end{Bmatrix}^{\mathrm{T}} \cdots \begin{Bmatrix} \boldsymbol{\delta}\mathbf{W}_i \\ \delta W_i \end{Bmatrix}^{\mathrm{T}} \cdots \begin{Bmatrix} \boldsymbol{\delta}\mathbf{W}_m \\ \delta W_m \end{Bmatrix}^{\mathrm{T}} \right]^{\mathrm{T}} \tag{7}$$

where $\Delta\mathbf{W}_i$ is the measured elemental MSEE change vector for the i^{th} mode and its components can be calculated directly from measured modal data and elemental stiffness matrix; ΔW_i is the measured total MSEE change for the i^{th} mode which can be calculated directly from measured modal data and system stiffness matrix; $\delta\mathbf{W}_i$ is the analytical elemental MSEE change vector for the i^{th} mode and its components can be estimated from Eq. (1); and δW_i is the analytical total MSEE change for the i^{th} mode which can be obtained by Eq. (4).

For the previously developed GMSEE method, only matching level between the patterns in the elemental GMSEE changes is considered. The constraint in this pattern is strengthened by using a good number of modes. Different from this method, the proposed MSEE method minimizes the dependence on the number of modes by utilizing an accurately estimated global parameter, the total MSEE change, as an additional constraint in the pattern of MSEE change vector. With this additional constraint, the identified damage vector must satisfy not only the pattern among the elemental MSEE changes but also the pattern among these individual components and the total MSEE changes. Therefore, a good estimation of damage vector can still be obtained with reduced number of modes.

As $\delta\mathbf{D}$ obtained from maximizing the MDLAC function described in Eq. (5) is a correlative vector, it means different scales of $\delta\mathbf{D}$ will give the same value of MDLAC. Therefore, the damage scaling coefficient, C, such that $C.\delta\mathbf{D}$ gives the actual damage extent in percentage, must be obtained. Based on the equation proposed for GMSEE,[11] the scaling coefficient C can be calculated using MSEE change as follows:

$$C = \frac{\sum_{i=1}^{m} \Delta W_i}{\sum_{i=1}^{m}\sum_{j=1}^{n} S_{ij}^{\text{avg}} \delta D_j} \tag{8}$$

where S_{ij}^{avg} is the average sensitivity of MSEE for the j^{th} element and the i^{th} mode obtained from the pre-damaged sensitivity S_{ij}^{u} calculated with modal information at undamaged state, and the post-damaged sensitivity S_{ij}^{d} calculated with modal information at damaged state.

Sensitivity-weighted search space (SWSS) scheme

As stated in the literature, the damage identification was found only reliable for elements with high strain energies. If the strain energy of an element is very small, damage in the element is unlikely to affect the behaviour of the structure. Conversely, the change in structural behaviour should be caused by change in structural properties of elements with high strain energy. For complex structures, because the number of measured modes may be much smaller than the number of elements, there might be many elements with low strain energies. As a result, significant false detection might be expected in the damage prediction results. Based on the idea of using modification function presented by Wahalathantri,[23] this section presents a new technique that can help to reduce false detection for correlation-based forward methods. Instead of adjusting the results with a modification function, the adjustment is applied to the search space.

Conventionally, search spaces for all elements are selected to be in the same range (e.g., from 0 to 100%). In other words, the high-sensitivity elements have the same range as the low-sensitivity elements. Therefore, the conventional range scheme may generate some false detections, especially when the measurement noise is significant and/or the number of DOFs is much greater than the number of measured modes.

It is worth noting that the low-sensitivity elements contribute little to the convergence of the objective function, and therefore, their importance should be treated differently from high-sensitivity elements in the optimization process. Considering the distribution of elemental MSE in all modes, a sensitivity-weighted search space (SWSS) scheme is developed for the correlation-based forward methods. As the sensitivity of elemental MSEE is in a form of MSE, it can be used to modify the traditional search space. The range for each element is defined based on its sensitivity as follows:

$$\delta D_j \in [0;100\%].\frac{S_j^{\text{mean}}}{\max(S_j^{\text{mean}})} \tag{9}$$

where δD_j is the damage extent variable of the j^{th} element, S_j^{mean} is the mean MSEE sensitivity of the j^{th} element to damage considering all measured modes; $\max(S_j^{\text{mean}})$ is the maximum value of the mean MSEE sensitivities. Using this scheme, the importance of an element is treated unequally with another element. The elements with high sensitivities have broader ranges, while the ones with low sensitivities have narrower ranges. The idea behind this scheme is that the high-sensitivity elements are allowed to vary more flexibly than the low-sensitivity elements; hence, the convergence of the objective function is more likely to be affected by the high-sensitivity elements. It is worth noting that damages in the low-sensitivity elements have little chances to be detected unless these damages are large enough. Although this scheme reduces detectability for the low-sensitivity elements, the damage identification results become more reliable as these elements usually cause ill-posed problem due to calculation errors or other uncertainties such as measurement noise.[20, 21] It is also worth noting again that the range of the damage extent variable does not represent the range of the damage. The final damage extent is the product of the optimal damage extent vector and the damage scaling coefficient described in Eq. (8).

Procedure of the MSEE correlation method incorporating with SWSS scheme is schematically shown in Fig. 1. Firstly, vibration responses of the structure at a baseline state and at the state that needs to be checked for its damage status are measured. Modal parameters such as natural frequencies and mode shapes are extracted from the vibration responses for each state. From the measured modal parameters and the elemental stiffness matrices, the measured MSEE change vector and the analytical MSEE change vector due to an arbitrary damage can then be calculated. Herein, the range of the damage vector is constrained based on the MSEE sensitivities according to the SWSS scheme. The GA optimization process is utilized to search for the optimal correlative damage vector that give the greatest MDLAC value. Finally, the damage extent is obtained after calculating the damage scaling coefficient *C*.

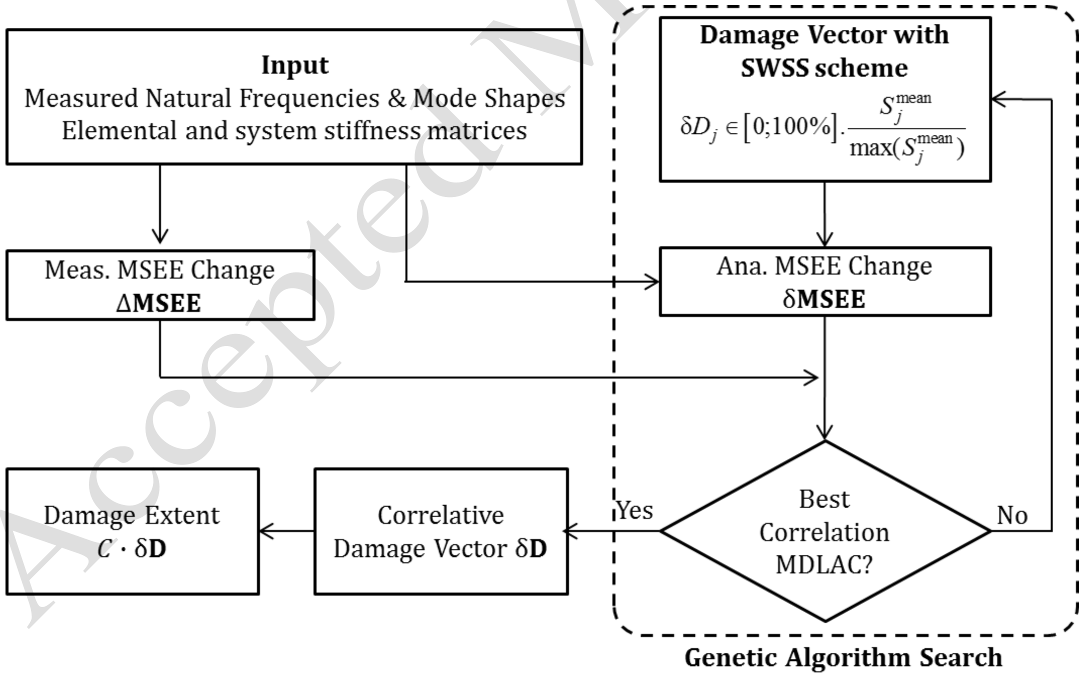

Figure 1. Schematic of proposed damage identification method

QUT through-truss bridge model

Description of test structure

As shown in Fig. 2, a steel through-truss bridge model was assembled at Banyo Pilot Plant Precinct of Queensland University of Technology (QUT), as a part of a previous PhD project on structural health monitoring.[24] The structure is a 3-span cantilever truss bridge model with a total length of 8.55m. The height of the main frame is 1.8m and the width of the bridge is 0.9m. The truss has 20 bays, each of which is 0.45m in length except the bays at two ends each of which has a length of 0.225m. Detailed dimensions are illustrated in Fig. 3. The structure consists of 198 nodes and 318 members of various cross sectional areas. The main structural members including chords, webs, struts and beams are made of cold formed mild steel with square/rectangular hollow sections. Meanwhile, the bracing members are steel flat bars. Detailed cross section and material properties for all members are listed in Table 1. The members in the main planes are jointed using bolt connection and steel gusset plates. The lateral struts and beams are also bolted to the gusset plates and the braces are bolted directly to the struts or beams. M6 bolts were used for most of the joints except the joints of the main frames where M8 bolts were used. In the healthy (original) condition, the M8 bolts were fastened to 10Nm and M6 bolts were fastened to 4Nm using a torque wrench. A pin in slotted hole was set at each far end of the bridge to simulate roller supports. A pin in fitted hole was set at the bottom of each main frame to simulate hinge support. In this study, one plane of the truss is considered for the damage identification experiment. The elements of the truss plane are numbered from 1 to 99 as shown in Fig. 4. It is worth noting that the number of elements to be examined in this study (i.e., 99 elements) is one of the largest numbers of elements that have been experimentally considered for research in this area.

Figure 2. QUT steel through-truss bridge model

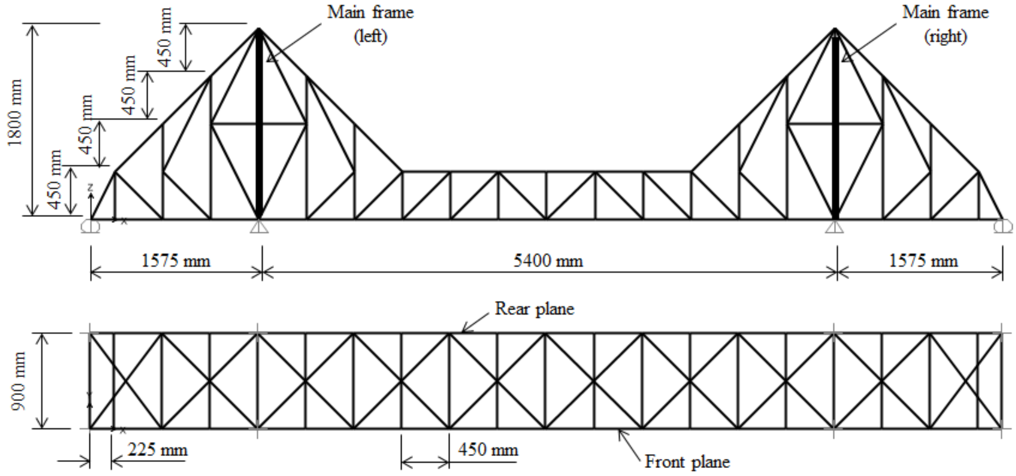

Figure 3. Dimensions of QUT steel through-truss bridge model

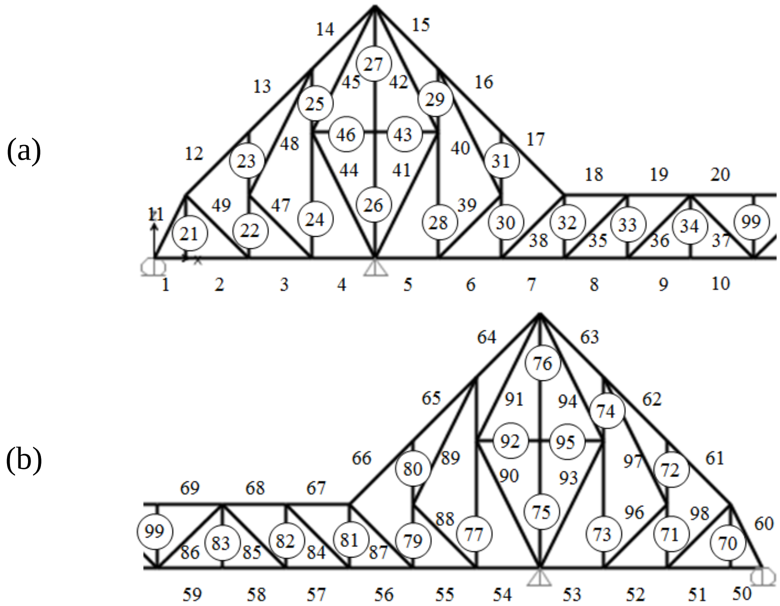

Figure 4. Element numbering for the examined truss plane of the QUT through-truss bridge model. (a) Left half of the examined truss plane; (b) Right half of the examined truss plane

Table 1. Details of structural members of QUT steel through-truss bridge model

Members	Section type	Dimension (mm)	Young's Modulus (GPa)	Mass density (kg/cm^3)
Top and bottom chords	Square hollow	20x20x1.6	200	7.85x10^3
Diagonals	Square hollow	20x20x1.6		
Vertical webs (at supports)	Square hollow	30x30x3.0		
Webs (others)	Square hollow	20x20x1.6		
Struts	Square hollow	20x20x1.6		
Beams	Rectangular hollow	50x25x2.0		
Braces	Flat bar	20x3.0		

Vibration Test

To measure vibration response of the examined plane of the bridge model, total 18 accelerometers including 14 PCB393B05 sensors with a nominal sensitivity of 10V/g and 4 PCB393B04 sensors with a nominal sensitivity of 1V/g were used. The first 14 accelerometers labelled from S1 to S14 are PCB393B05 type and the rest labelled from S15 to S18 are PCB393B04 type. A chassis NI cDAQ-9172 embedded with five DSA modules NI-9234 with 4 channels in each was used to capture the signals from the accelerometers. In order to achieve precise synchronization across different modules, programming was done using LabVIEW to ensure that all the DSA modules share one time base source.[25]

A roving test method was designed to capture the responses of most of the DOFs in the examined plane of the truss model. As shown in Fig. 5, six (6) sensor layouts were designed in which 17 sensors were roved along the truss length and one sensor was used as the reference (i.e., sensor S2). As modal strain energy of each element is calculated from mode shapes of 4 DOFs at its ends, redundant DOFs were measured for some important elements at the 8th and 12th bays as shown in Fig. 5(f) to reduce the uncertainty associated with multiple measurements. The structure was excited by a hammer at the joint next to the mid span joint (i.e., the joint of the 9th and 10th bays). The sampling rate was set as 512Hz and the duration of measurement for each layout was set as 2 minutes. Totally, vibration responses of 88 DOFs over 100 DOFs of the truss plane were measured. Later, modal features of the unmeasured 12 DOFs were estimated from the measured ones using the linear interpolation method. Figure 6 shows the photos of sensors at some typical joints of the bridge model.

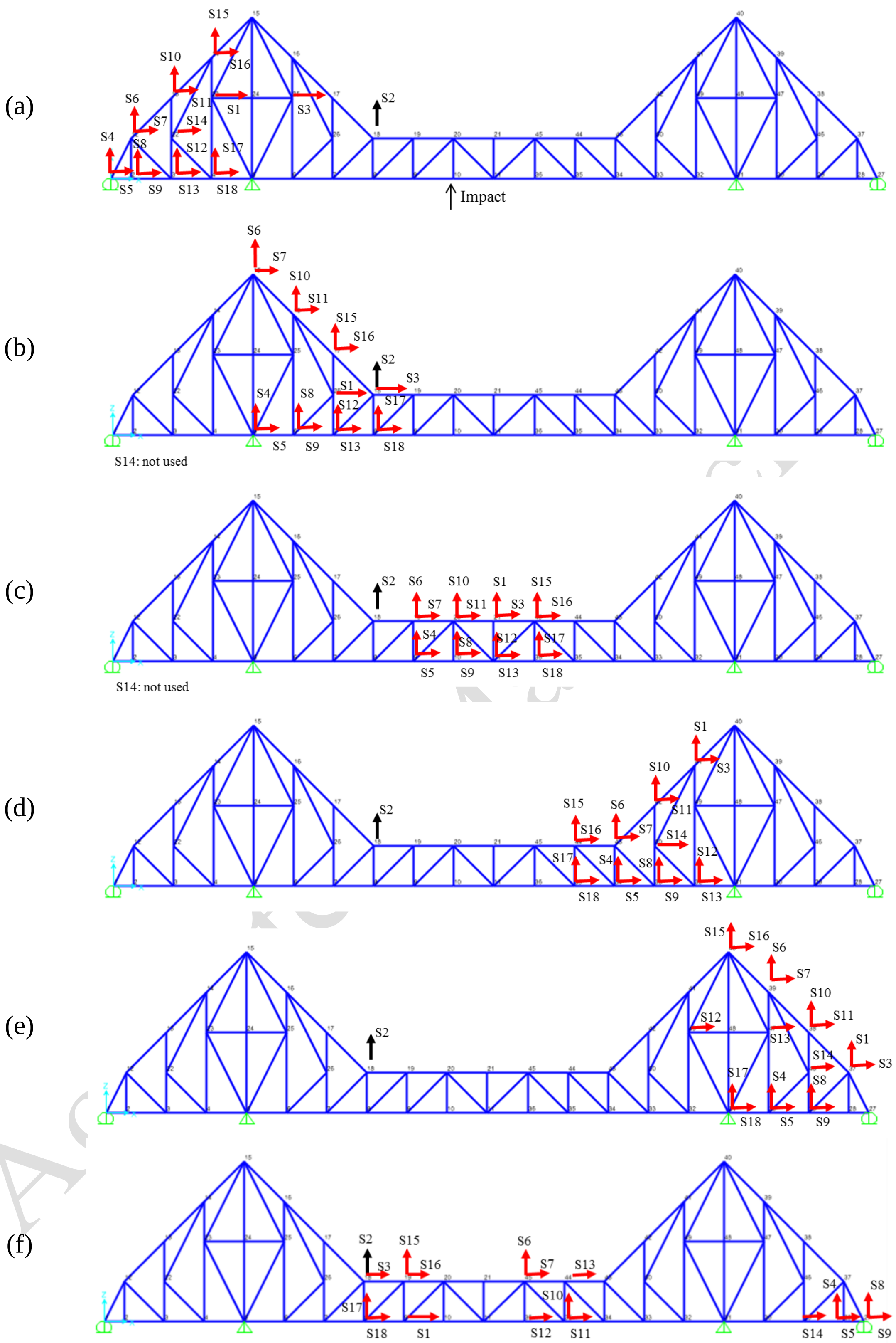

Figure 5. Sensor layouts for vibration measurement of the QUT through-truss bridge model. (a) Layout 1; (b) Layout 2; (c) Layout 3; (d) Layout 4; (e) Layout 5; (f) Layout 6.

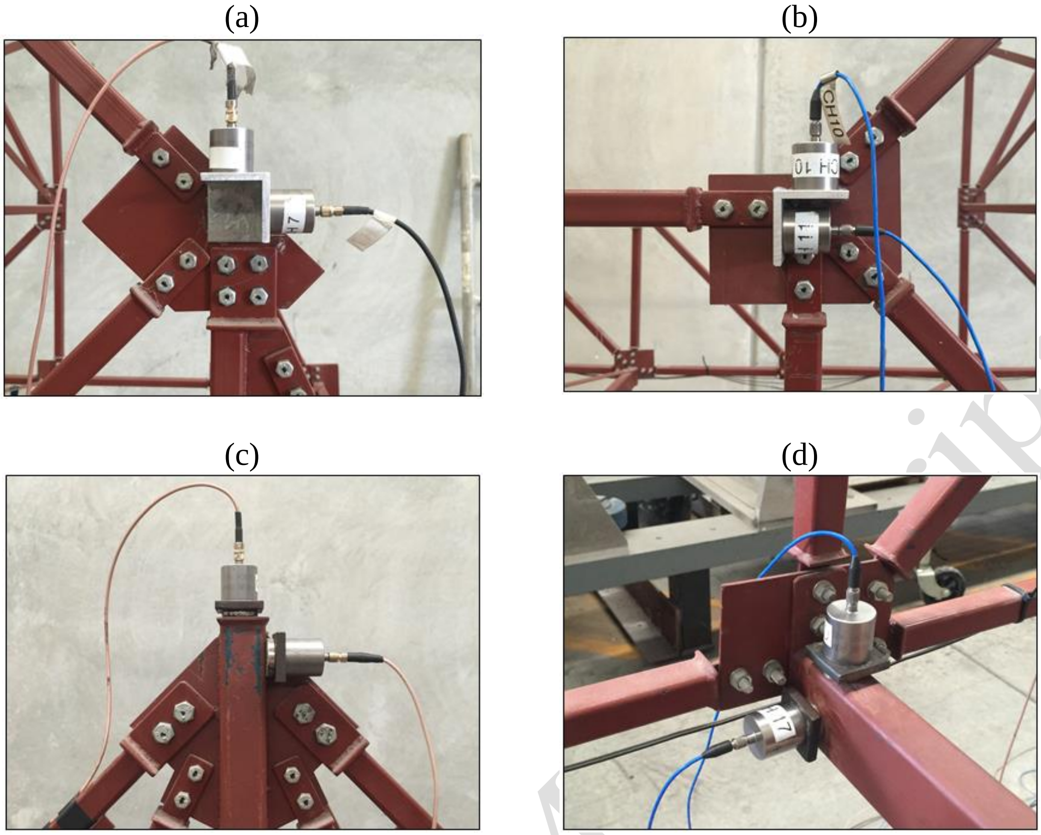

Figure 6. Sensors at some typical joints of the QUT through-truss bridge model. (a) at joint of 2 inclined-top chords, (b) at joint of inclined chord-horizontal chord, (c) at top of a main frame, (d) at joint of bottom chords.

Modal extraction and mode selection

The modal analysis software package ARTeMIS Extractor Pro version 5.3 developed by Structural Vibration Solution A/S was used to process vibration data from the truss structure. The frequency domain decomposition (FDD) method embedded in ARTeMIS was used to extract modal information such as natural frequencies and mode shapes. As the signals were sampled at 512Hz, the frequency range of interest is from 0 to 256Hz. The number of frequency point was set as 2048 that gave the frequency resolution to be 0.125Hz. It should be noted only the values from 0 to about the first half of the frequency range are considered as they are more reliable for mode shape estimation. It is also worth noting that the frequency resolution can be finer by increasing the number of frequency point. However, this makes the singular value decomposition (SVD) diagrams very noisy and it is very hard to pick the modes.

Figure 7 shows the SVD diagrams for the vibration data of all the test layouts in the baseline condition. Natural frequencies of the truss plane can be identified from the peaks of the first

SVD diagram and corresponding mode shapes can be estimated. As shown in Fig. 7, there are many peaks, but not all of them can be used for damage identification. Some peaks represent local modes due to local vibration of individual elements. Some peaks are not stable due to the nonlinearity of the structure or due to the uncertainties of the roving test (such as the reference sensor is close to nodal point of these modes). In order to select appropriate modes for damage identification, the following criteria are applied: firstly, the mode must have a low mode shape complexity that represents a true mode; secondly, the mode must have a good repeatability in modal strain energy for different data sets in the same structural condition; and thirdly the mode must represent global behavior of the structure.

For the first criterion, the mode shape complexity represents the effect of non-proportional damping. It has been reported that mode shape complexity increases with bias and random error on mode shape estimates.[26] Therefore, in this study, the modes with complexity values greater than 20% are neglected.

For the second criterion, the modal assurance criteria of modal strain energy (MAC_{MSE}) are calculated for the modes that satisfy the first criterion, and then the modes with MAC_{MSE} value greater than 95% are selected. The equation of MAC_{MSE} is as follows:

$$MAC_{MSE}(i) = \frac{\left(\mathbf{MSE}_{i,1}^{T}.\mathbf{MSE}_{i,2}\right)^{2}}{\left(\mathbf{MSE}_{i,1}^{T}.\mathbf{MSE}_{i,1}\right).\left(\mathbf{MSE}_{i,2}^{T}.\mathbf{MSE}_{i,2}\right)} \tag{10}$$

where $\mathbf{MSE}_{i,1}$ is the first data set of the i^{th} MSE data of the structure, and $\mathbf{MSE}_{i,2}$ is the second data set of the i^{th} MSE data of the structure.

The third criterion is applied to avoid local modes. We consider a good MSE distribution must contain a good number of high MSE values. The quality of the MSE distribution can be evaluated by the ratio of number of MSE values greater than the mean value over the total number of MSE values, as follows:

$$p_{\mathrm{MSE}} = \frac{n_{\mu}}{N} \times 100\% \tag{11}$$

where n_{μ} is the number of MSE values being greater than the mean value of MSE distribution and N is the number of MSE values (e.g., $N = 99$ for this truss structure). In this study, only the modes with at least 20% of MSE values greater than the mean value (i.e., $p_{\mathrm{MSE}} \geq 20\%$) are selected. It is worth noting that this criterion was set as a result of trade-off between the number of modes and the quality of the MSE distribution.

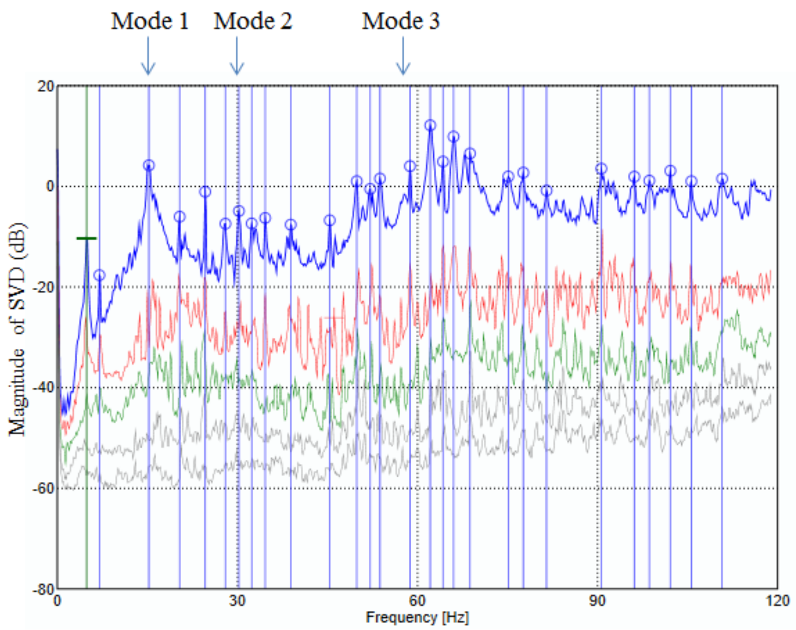

Figure 7. SVD diagram and the identified natural frequencies for the QUT through-truss bridge model

Table 2 shows the summary of modal characteristics of all the peaks selected from the SVD diagram. It can be seen that only three modes (i.e., 15.375 Hz, 30.25 Hz and 58.75 Hz) satisfy all the three criteria above. These modes are respectively marked as mode 1, mode 2 and mode 3 in the SVD diagram of Fig. 7. An example of MSE of an unselected mode (7 Hz) that does not satisfy the repeatability requirement (criterion 2) is shown in Fig. 8; and an example for an unselected mode (62.125 Hz) that does not satisfy the global behaviour requirement (criterion 3) is shown in Fig. 9. It is clearly seen in Fig. 8 that the 7-Hz mode is not a stable mode as its MSE diagrams from two data sets are significantly different. As shown in Fig. 9, the 62.125-Hz mode represents a local mode where the response of one element (i.e., element 50) dominates the responses of other elements. Figure 10 shows the MSE diagrams of the three selected modes (modes 1-3). It is obvious that these modes have good repeatability and well represent global behaviours. Figure 11 shows the mode shapes associated with the identified modes. For verification, mode shapes of a finite element (FE) model of the truss bridge established with SAP2000 software package are also plotted in Fig. 11. It can be found that the experimental modes match very well with the modes calculated from the FE model. Differences in the natural frequencies between the experimental model and FE model are very small, up to only 2%. By comparing with the numerical mode shapes, the first two measured modes might represent in-plane bending behaviours and the third measured mode might represent torsional behaviour. Despite the visual similarity in mode shapes, the modal assurance criterion (MAC) values are found as 0.653, 0.304 and 0.598 for modes 1-3, respectively, indicating significant differences in structural properties of individual elements between the FE model and the experimental model. For the traditional forward methods that heavily rely on numerical model (e.g., mode shape-based method[6] or MSE-based method[7]), this FE model will need intensive model updating and this may be a challenging task. This case clearly shows the advantage of the MSEE method over the traditional methods as it does not require a numerical model.

Table 2. Summary of mode selection for the QUT through-truss bridge model

Peak Freq. (Hz)	Criterion 1 (C1): Complexity		Criterion 2 (C2): Repeatability		Criteron 3 (C3): Global behavior	
	Comp. (%)	C1-Pass	MAC_{MSE}	C2-Pass	p_{MSE} (%)	C3-Pass
4.875	76.0		-		-	
7.000	12.9	✓	0.42		-	
15.375	0.4	✓	0.99	✓	22.2	✓
20.375	48.2		-		-	
24.625	94.8		-		-	
28.000	27.8		-		-	
30.250	12.3	✓	0.98	✓	24.2	✓
32.375	46.8		-		-	
34.625	28.5		-		-	
38.875	83.6		-		-	
45.375	39.0		-		-	
49.875	93.9		-		-	
52.125	56.0		-		-	
53.750	34.9		-		-	
58.750	12.6	✓	0.98	✓	30.3%	✓
62.125	6.9	✓	1.00	✓	15.2%	
64.250	13.7	✓	0.92		-	
66.000	59.6		-		-	
68.750	10.0	✓	0.99	✓	18.2%	
75.125	59.8		-		-	
77.625	27.0		-		-	
81.500	88.0		-		-	
90.625	70.4		-		-	
96.125	65.1		-		-	
98.625	64.5		-		-	
102.125	58.6		-		-	
105.625	57.2		-		-	
110.750	45.9		-		-	

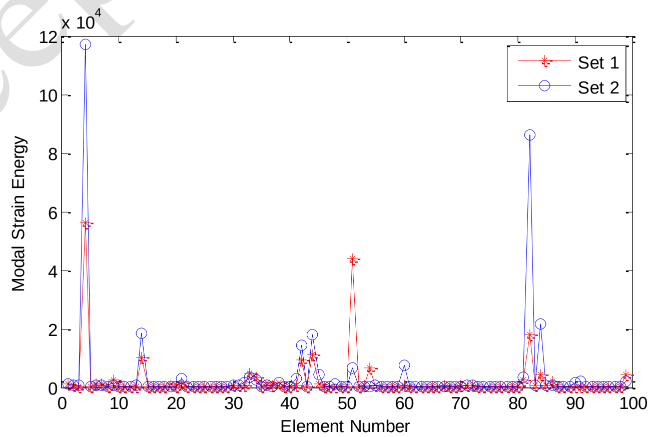

Figure 8. Modal strain energy of the unselected mode at 7Hz from two different data sets

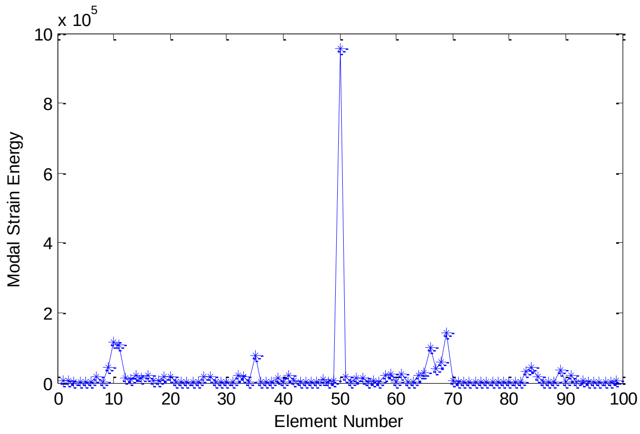

Figure 9. Modal strain energy of the unselected mode at 62.125Hz

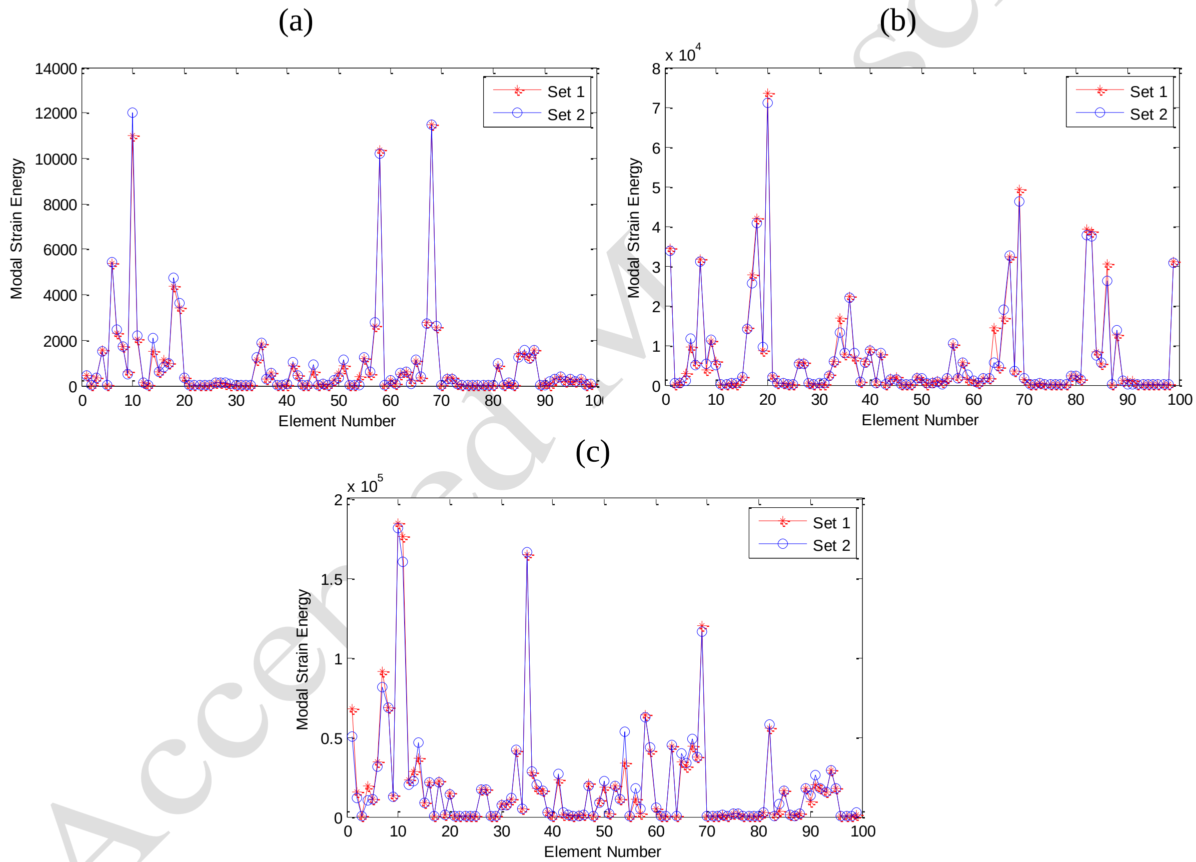

Figure 10. Modal strain energy for the selected mode from 2 different data sets. (a) Mode 1: 15.375Hz; (b) Mode 2: 30.25 Hz; (c) Mode 3: 58.75Hz

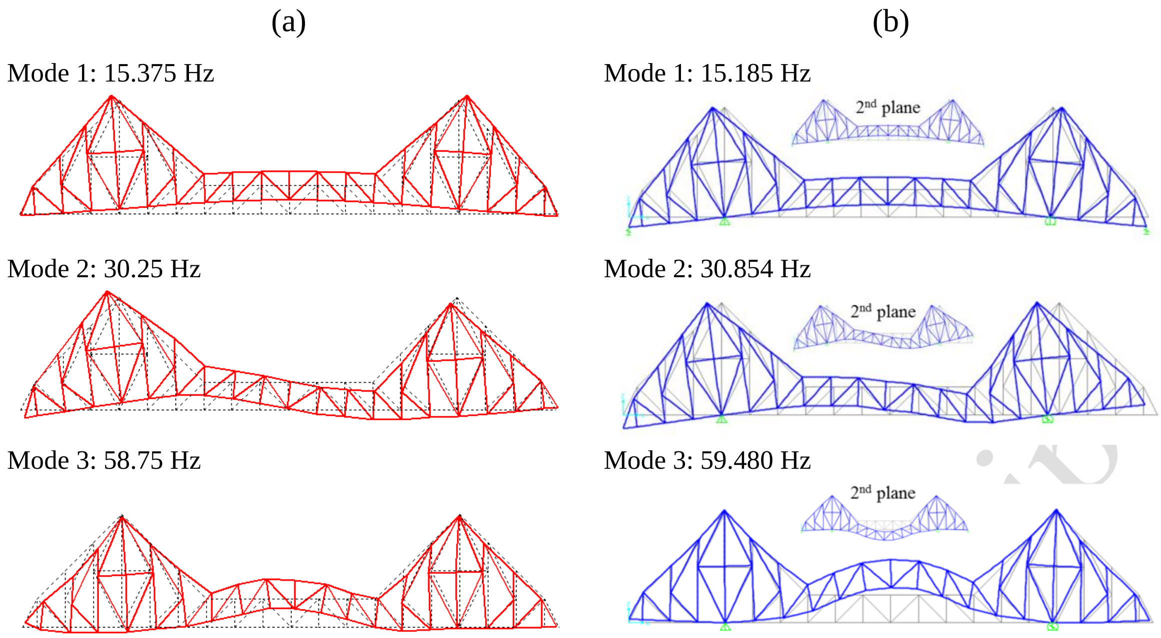

Figure 11. Mode shapes of the QUT through truss bridge model. (a) Experiment; (b) FEM

Damage identification for the QUT through truss bridge model

Damage scenarios

The failure of joints (e.g. welds or bolts) is one of the typical damages in steel truss structures.[27] For bolted joints, there is a high possibility that some bolts are loosened or even removed from the structure.[18] For a truss member, stiffness of the whole member is dependent not only on the truss bar's stiffness but also on the joint stiffness. Figure 12 shows a physical model of a bolted truss element, consisting of axial stiffness of the truss bar and stiffness of the joints. The joint stiffness represents the tangential contact stiffness of the bolts, and this value is proportional to contact pressure caused by bolt torque.[28] The equivalent stiffness of the member, k_e, can be expressed as follows:

$$\frac{1}{k_e} = \frac{1}{k_{\text{joint-1}}} + \frac{1}{k_{\text{joint-2}}} + \frac{1}{k_{bar}} \quad (12)$$

where $k_{\text{joint-1}}$ and $k_{\text{joint-2}}$ refer to the joint stiffness constants at each end of the truss bar; k_{bar} is the axial stiffness of the bar itself. When all bolts are fully fastened ($k_{\text{joint-1}} = k_{\text{joint-2}} = \infty$), the equivalent stiffness of the member is equal to k_{bar}. When some bolts are partially loosened, the equivalent stiffness will reduce. When the bolts at either end are fully loosened ($k_{\text{joint-1}} = 0$ or

$k_{\text{joint-2}} = 0$), the equivalent stiffness become vanish or the member is totally failed. It is worth noting that the stiffness of the joint is also affected by many other factors such as surface roughness, elasticities and contact area;[28] and these factors are hard to be controlled. Therefore, in this study, only the existence of damage and the increasing trend of damage are examined.

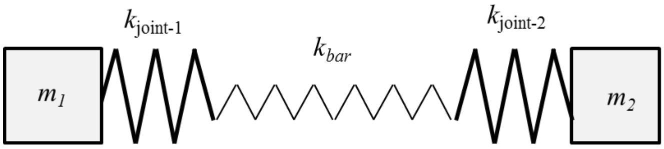

Figure 12. Spring-in-series model of bolted truss element

Various bolt loosening scenarios are considered in this study, as summarized in Table 3. Test 1 refers single damage at member 10 with two levels of damage severity. In the first damage state, bolts at one end of member 10 were loosened to hand tightening level (approximate 0.5Nm torque). In the second damage state, all bolts were loosened to hand tightening level. Test 2 refers two damages at members 7 and 67 in which all the bolts of these members were loosened to hand tightening level. Figure 13 illustrates the positions of the damaged elements considered in these tests. Table 4 summarizes the natural frequencies of the truss bridge model for the two undamaged states and three damaged states. It can be seen that the changes in natural frequencies are not very noticeable. For the first test, only the first natural frequency slightly reduced after all the bolts of element 10 were loosened. For the second test, only slight change is observed in the natural frequency of mode 2. These small changes in natural frequencies are reasonable considering the structure is very large and the contribution of each individual member on the overall behaviour of the structure is very small. To clarify this point, a damage of 20% in element 10 (similar to state 1-1) is simulated in the FE model. The changes in the first three numerical frequencies are very small of about 0.033Hz (0.22%), 0.042Hz (0.14%) and 0.048Hz (0.09%), respectively. These changes are even much smaller than the frequency resolution (0.125Hz) in the experimental study.

Table 3. Damage scenarios for the QUT through-truss bridge structure

Test	State	Description
Test 1	State 1-0	Undamaged
	State 1-1	#10: bolts at one end loosened to hand tightening (~0.5Nm)
	State 1-2	#10: bolts at two ends loosened to hand tightening (~0.5Nm)
Test 2	State 2-0	Undamaged: bolts refastened to healthy condition (~4Nm)
	State 2-1	#7 and #67: bolts at two ends loosen to hand tightening (~0.5Nm)

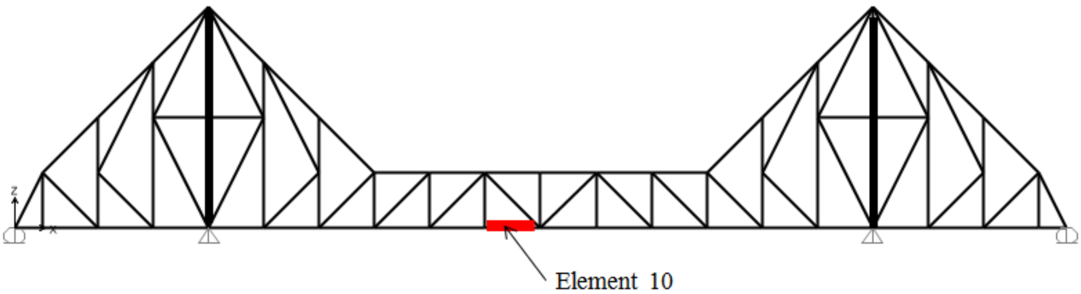

(a) State 1-1 and State 1-2

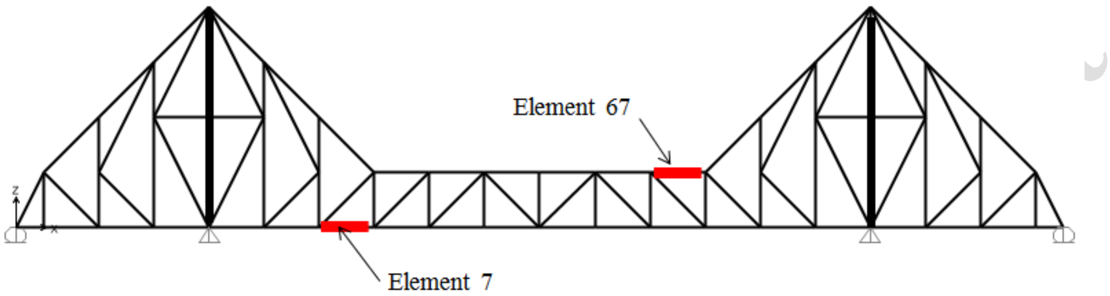

(b) State 2-1

Figure 13. Illustration of damaged elements on the QUT through-truss bridge model

Table 4. Natural frequencies of the QUT through-truss bridge structure at undamaged and damaged states

Test	State	Natural frequency (Hz)		
		Mode 1	Mode 2	Mode 3
Test 1	State 1-0	15.375	30.250	58.750
	State 1-1	15.375	30.250	58.750
	State 1-2	15.250	30.250	58.750
Test 2	State 2-0	15.250	30.250	58.750
	State 2-1	15.250	30.125	58.750

Damage identification

In this study, the GA optimization toolbox embedded in MATLAB software package is utilized to solve the optimization problem described by Eq. 5. The solver parameters are set as follows. The number of variables is 99 corresponding to the total number of truss elements under consideration. The population size is 500 as of about five times of the number of the dimensions (i.e., 99). The crossover fraction rate does not need to be very high since a large population size has been defined, so it is set as 0.5. The convergence tolerance is used as a condition to stop the GA process and it is set as 1e-10. As this is a constrained optimization problem, the adaptive feasible mutation function integrated in the toolbox is used for generating mutated individuals.

Conventionally, the range of the damage variables can be set equally for all elements (e.g., from 0 to 1). However, due to high uncertainty associated with complex structures, low number of modes and potential measurement noise induced from roving test, the SWSS scheme presented previously (Eq. 9) is applied for this structure. Figure 14 shows the search spaces of all elements based on the SWSS scheme. Only some elements have wide ranges with upper bound of over 0.5, such as elements 10, 20 and 69. A good number of elements have medium ranges with the upper bound varying from 0.1 to 0.5, such as elements 6, 36 and 65. Moreover, many elements have very narrow ranges with the upper bound of under 0.1, such as elements 2, 3 and 11. For detailed locations of the element, please refer to Fig. 4.

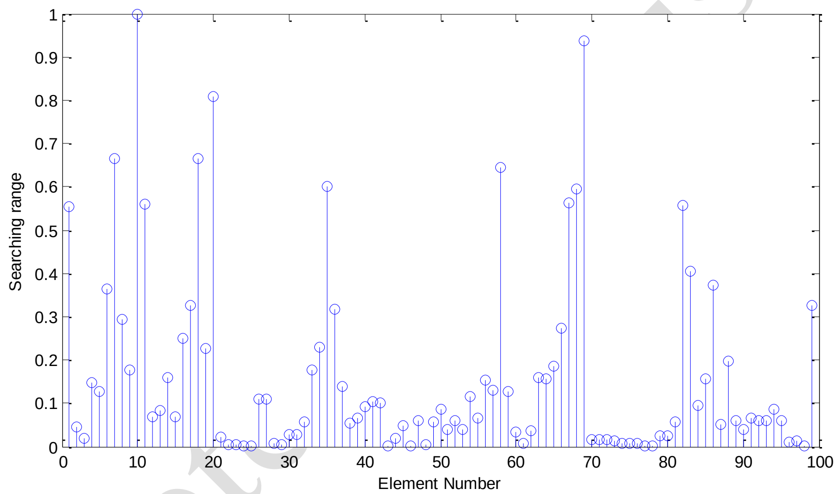

Figure 14. Sensitivity-weighted search space of all elements of the examined plane of the QUT through-truss bridge model

Damage identification results by the MSEE correlation method with the conventional equal search space is shown in Fig. 15. It is shown that the method can clearly detect the actual damage (element 10) for the single damage states (States 1-1 and 1-2). Although there is a few false detection errors, element 10 has much higher possibility of damage. Also, the method is successful to show the increase of damage in element 10. For the double damage state (State 2-1), although the method with conventional search space can show the actual damaged elements 7 and 67, there are plenty of false positive errors with similar possibility of damage as those of the actual damaged elements. It is found that many of these false elements have very small sensitivities by referring the diagram in Fig. 14.

Damage identification results by the MSEE correlation method with the enhanced technique SWSS is shown in Fig. 16. It can be seen that the damage results are significantly improved. For single damage states, damage at element 10 is clearly predicted in both states and its damage increase is well captured. There are still a few false errors in the results but their severities are less than those obtained from the conventional search space. For the double damage state, false errors are significantly reduced, and the damages at element 7 and 67 are more readily to be identified as their severities are well distinguished from those of the false members.

For decision making about damage location, multiple thresholds can be defined corresponding to different levels of safety. In this study, two thresholds of 5% and 10% are considered. It is worth noting that, damage is identified with higher confidence using the higher threshold but it may ignore some possible small damage. Meanwhile, the lower threshold may give higher safety state but the decision of damage becomes less confident. It is worth noting that, in real application, the confidence level for a damage threshold can be identified by statistical analyses using long-term monitoring data.[29-30] Table 5 summaries the prediction results obtained by the MSEE correlation method with the equal range search space and with SWSS. By setting the threshold as 5%, the false elements are taken into account for about 2-4% of all elements with the equal range search space for the single damage states. The percentages of false elements decrease a little by using the SWSS. For the double damage state, about 13% of location errors are obtained by using the conventional search space, whereas only 2% of location errors are found by using the SWSS method. By setting the threshold as 10%, some false errors are still observed for State 1-1 and 1-2 using the conventional search space. Meanwhile, only one false error is identified at element 99 in State 1-2 using the SWSS. However, this damage seems not to be an error as element 99 is adjacent to the actual damaged element 10. It can be expected that damage in a truss element might change the orientation and/or force distribution of the adjacent elements. For State 2-1 with the threshold of 10%, a large portion of location error is still obtained by using the conventional search space, whereas no false error is found by using the SWSS.

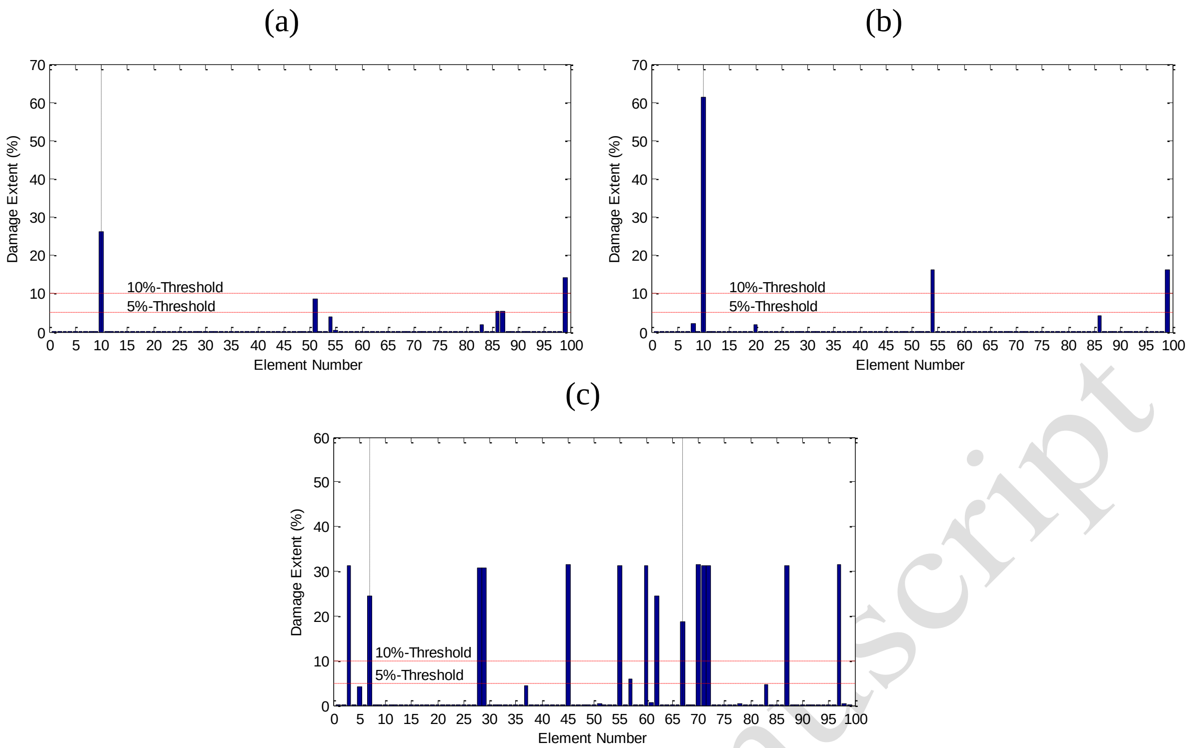

Figure 15. Damage identification results using MSEE method with equal search space. (a) State 1-1; (b) State 1-2; (c) State 2-1.

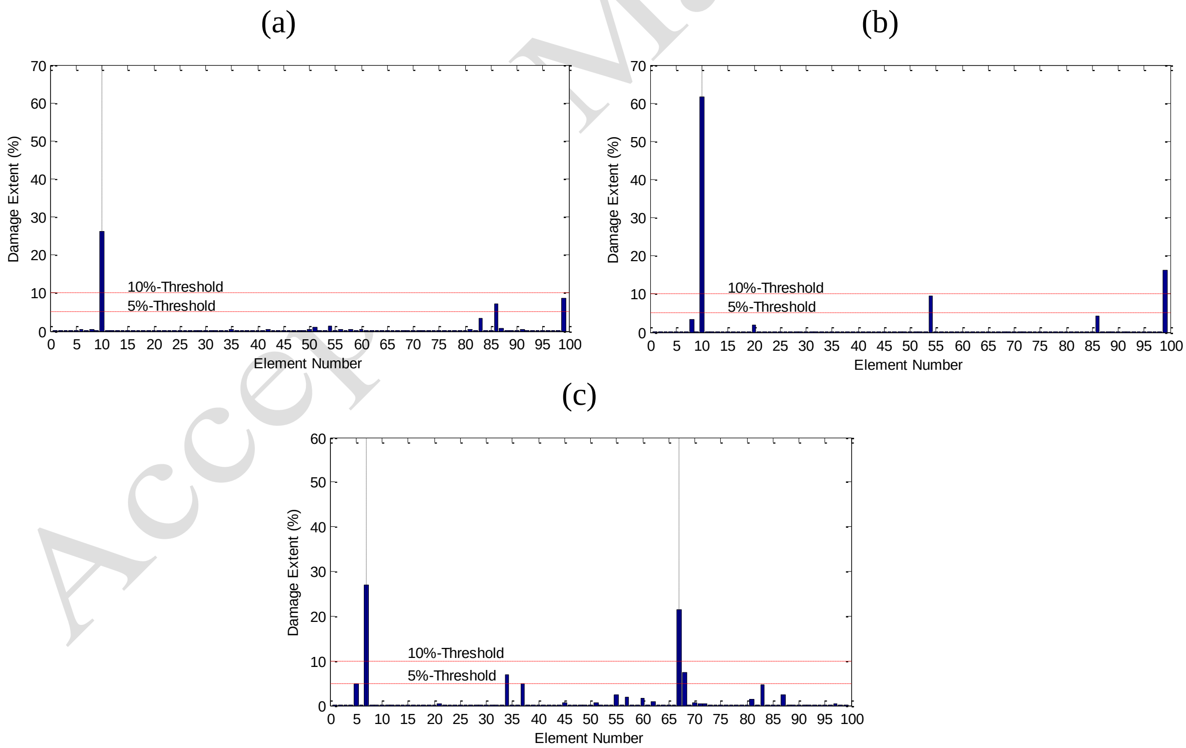

Figure 16. Damage identification results using MSEE method with SWSS. (a) State 1-1; (b) State 1-2; (c) State 2-1.

Table 5. Damage location results for the QUT through-truss bridge model

State	Damaged Elements	MSEE and equal range search space	Loc. false error (%)	MSEE and SWSS	Loc. false error (%)
5% Threshold					
State 1-1	10	10, 51, 86, 87, 99	4%	10, 86, 99	2%
State 1-2	10	10, 54, 99	2%	10, 54, 99	2%
State 2-1	7, 67	3, 7, 28, 29, 45, 55, 57, 60, 62, 67, 70, 71, 72, 87, 97	13%	7, 34, 67, 68	2%
10% Threshold					
State 1-1	10	10, 99	1%	10	0%
State 1-2	10	10, 54, 99	2%	10, 99	1%
State 2-1	7, 67	3, 7, 28, 29, 45, 55, 60, 62, 67, 70, 71, 72, 87, 97	12%	7, 67	0%

The above damage results have been obtained from the signals with some redundant channels at the 8th and 12th bays (see Fig. 5(f)). It is interesting to see whether these redundant channels are necessary for the damage identification problem. Figure 17 shows the damage identification results using the MSEE method and SWSS but without considering the redundant channels. For the low damage level of element 10 (State 1-1), the number of location false errors increases if we consider a threshold of 5%. One significant false error is found at element 18. The lack of redundant channels seems not to affect to the result of State 1-2 as it is comparable to the one with redundant channels. For the double damage state (State 2-1), the damage extents of elements 7 and 67 are very low and cannot be identified as damage. Also, two significant false errors are found at elements 18 and 85. It is worth noting that elements 18 and 85 have high sensitivities (as shown in Fig. 14) that mean they have high impacts in the damage identification process. However, their MSEs are calculated from two consequent layouts 2 and 3 (see Fig. 5 (b) and (c)) since the redundant channels are not considered. Therefore, calculation errors are expected and this leads to the poor damage identification results. From this analysis, it is recommended to set up redundant channels (at least for the elements of high sensitivities) in roving tests for more reliable damage identification results.

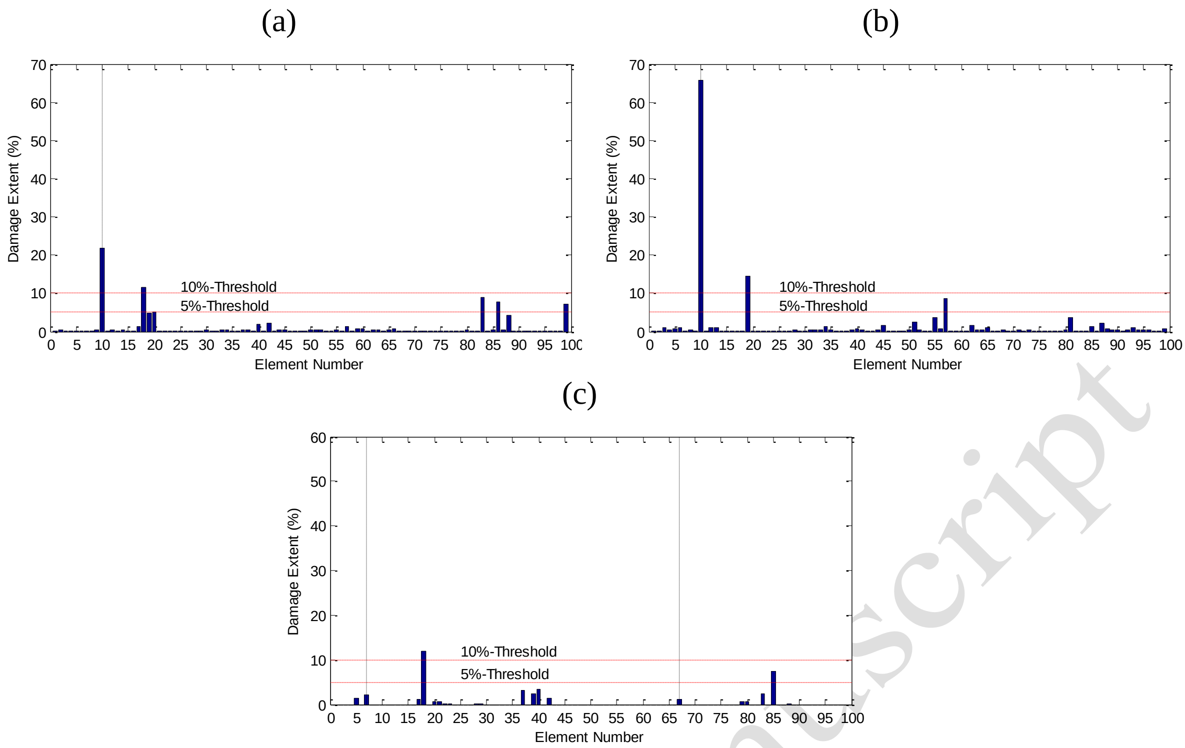

Figure 17. Damage identification results using MSEE method with SWSS regardless redudant channels. (a) State 1-1; (b) State 1-2; (c) State 2-1.

Conclusions

This paper presented methodology development and application on damage identification for a complex truss structure using an improved correlation-based algorithm incorporating with a new search space scheme. As a modification of a recently developed GMSEE method, the improved correlation-based algorithm named MSEE method considers both elemental MSEE and total MSEE to better reflect the damage effect. Compared to the traditional optimization-based methods using mode shape change or MSE change, the MSEE method does not rely on numerical model and this make it more practical for complex structures. To enhance the performance of the MSEE method, the new search space scheme named SWSS was introduced in which different search space ranges are applied to different structural elements based on their MSEE sensitivity. For validation, vibration tests on a complex truss structure were conducted using a sensor roving method. Six sensor layouts were designed to estimate mode shapes of 100 DOFs of the test structure. Some redundant sensors were set up to refine modal strain energy values of some important elements. A three-step mode selection approach was proposed to select appropriate vibration modes out of many potential modes estimated by the FDD method. Single damage and multiple damage scenarios were designed by loosening bolts.

From the experimental results, it was found that the MSEE method incorporating with SWSS scheme can effectively identify damage in the truss structure. All the actual damaged elements were accurately detected. Also, the increment of damage was successfully captured. Regarding false detection, only about 2% of all elements were falsely detected using the threshold of 5% and almost no false elements were observed with the threshold of 10%. Besides, the results demonstrated the effectiveness of the SWSS scheme as it helped to reduce a significant amount of false detection errors. By examining the damage results without the redundant accelerometers, it was found that damage identification errors (either false positive or false negative errors) tended to increase if these sensors were ignored. For measurement using sensor roving method, therefore, it is recommended to have redundant sensors at the elements of high sensitivities in order to reduce measurement uncertainty. The future research will treat the validation of the proposed method for real complex structures and for different types of structural damage.

Acknowledgements

The first author would like to express his sincere appreciation to Queensland University of Technology (QUT) for the financial support for his research. Gratitude is also given to researchers and staff members at Banyo Pilot Plan Precinct of QUT for providing facilities and helps for the vibration test on the truss model.

References

1. Farrar CR and Doebling SW. An overview of modal-based damage identification methods. Proc. of DAMAS conference, Sheffield, UK, 1997.
2. Rytter, A. Vibration based inspection of civil engineering structural, PhD Dissertation, Aalborg University, Denmark, 1993.
3. Pandey AK and Biswas M. Damage detection in structures using changes in flexibility. *Journal of Sound and Vibration* 1994; 169: 3-17.
4. Kim JT, Ryu YS, Cho HM and Stubbs N. Damage identification in beam-type structures: frequency-based method vs mode shape-based method. *Engineering Structures* 2003; 25: 57-67.

5. Messina A, Williams E and Contursi T. Structural damage detection by a sensitivity and statistical-based method. *Journal of Sound and Vibration* 1998; 216: 791-808.
6. Shi ZY, Law SS and Zhang LM. Damage localization by directly using incomplete mode shapes. *Journal of Engineering Mechanics* 2000; 126: 656-660.
7. Shi Z Y, Law SS and Zhang LM. Structural damage detection from modal strain energy change. *Journal of Engineering Mechanics* 2000; 126: 1216–1223.
8. Koo KY, Sung SH and Jung HJ. Damage Quantification of Shear Buildings Using Deflections Obtained by Modal Flexibility. *Smart Materials and Structures* 2010; 20(4): 1-9.
9. Bayissa WL and Haritos N. Damage identification in plate-like structures using bending moment response power spectral density. *Structural Health Monitoring* 2007; 6(1): 5-20.
10. Bandara RP, Chan THT and Thambiratnam DP. Structural damage detection method using frequency response functions. *Structural Health Monitoring* 2014; 13(4): 418-429.
11. Nguyen KD, Chan THT and Thambiratnam DP. Structural damage identification based on change in geometric modal strain energy-eigenvalue ratio. *Smart Materials and Structures* 2016; 25: 14pp.
12. Farrar CR, Baker WE, Bell TM, Cone KM, Darling TW, Duffey TA, Eklund A and Migliori A. Dynamic characterization and damage detection in the I-40 bridge over the Rio Grande. Report: LA-12767-MS, Los Alamos National Laboratory, NM, USA, 1994.
13. Abdel Wahab MM and De Roeck G. Damage detection in bridges using modal curvatures: application to a real damage scenario. *Journal of Sound and Vibration* 1999; 226(2): 217-235.
14. Liu PL. Identification and damage detection of trusses using modal data. *Journal of Structural Engineering* 1995; 121(4): 599-608.
15. Shih HW, Thambiratnam DP and Chan THT. Damage detection in truss bridges using vibration based multi-criteria approach. *Structural Engineering and Mechanics* 2011; 39(2): 187-206.
16. Wang FL, Chan THT, Thambiratnam DP, Tan ACC and Cowled CLJ. Correlation-based damage detection for complicated truss bridges using multi-layer genetic algorithm *Advances in Structural Engineering* 2012; 15: 693-706.
17. Montazer M and Seyedpoor SM. A new flexibility based damage index for damage detection of truss structures. *Shock and Vibration* 2014; 2014: 12pp.

18. An Y, Li B and Ou J. An algorithm for damage localization in steel truss structures: Numerical simulation and experimental validation. *Journal of Intelligent Material Systems and Structures* 2013; 24(14): 1683-1698.
19. Lee SG, Yun GJ and Shang S. Reference-free damage detection for truss bridge structures by continuous relative wavelet entropy method. *Structural Health Monitoring* 2014; 13(3): 307-320.
20. Salawu OS. Detection of structural damage through changes in frequency: a review. *Engineering Structures* 1997; 19(9): 718-723.
21. Salane H and Baldwin J. Identification of modal properties of bridges. *Journal of Structural Engineering* 1990; 116(7): 2008-2021.
22. Hsu TY and Loh CH. Damage diagnosis of frame structures using modified modal strain energy change method. *Journal of Engineering Mechanics* 2007; 134(11): 1000-1012.
23. Wahalathantri BL. Damage assessment in reinforced concrete flexural members using modal strain energy based method. PhD Dissertation, Queensland University of Technology. 2012.
24. Cowled CJL, Thambiratnam DP, Chan THT and Tan ACC. Structural complexity in structural health monitoring: Preliminary experimental modal testing and analysis. Proc. of the 7th World Congress on Engineering Asset Management (WCEAM 2012), Daejeon, South Korea, 2015.
25. Nguyen T, Chan THT and Thambiratnam DP. Effects of wireless sensor network uncertainties on output-only modal analysis employing merged data of multiple tests. *Advances in Structural Engineering* 2014; 17(3): 319-329.
26. Brincker R and Ventura C. *Introduction to operational modal analysis*. Chichester, West Sussex: John Wiley & Sons, 2015.
27. Merjoo M, Khaji N, Moharrami H and Bahreininejad A. Damage detection of truss bridge joints using Artificial Neural Networks. *Expert Systems with Applications* 2008; 35: 1122-1131.
28. Kartal ME, Mulvihill DM, Nowel D and Hills DA. Measurements of pressure and area dependent tangential contact stiffness between rough surfaces using digital image correlation. *Tribology International* 2011; 44: 1188-1198.
29. Xia Y, Hao H, Brownjohn JMW and Xia PQ. Damage identification of structures with uncertain frequency and mode shape data. *Earthquake Engineering and Structural Dynamics* 2002; 31: 1053-1066.

30. An Y, Jo H, Spencer BF and Ou J. A damage localization method based on the ‘jerk energy’. *Smart Materials and Structures* 2014; 23: 1–14.